Enhanced magnetic ordering in Sm metal under extreme pressure

Y. Deng and J. S. Schilling

Department of Physics, Washington University, St. Louis, Missouri 63130, USA

The dependence of the magnetic ordering temperature T_o of Sm metal was determined through four-point electrical resistivity measurements to pressures as high as 150 GPa. A strong increase in T_o with pressure is observed above 85 GPa. In this pressure range, Sm ions alloyed in dilute concentration with superconducting Y exhibit giant Kondo pair breaking. Taken together, these results suggest that for pressures above $\sim$85 GPa Sm is in a highly correlated electron state, like a Kondo lattice, with an unusually high value of T_o. A detailed comparison is made with similar results obtained earlier on Nd, Tb, and Dy and their dilute magnetic alloys with superconducting Y.

I. INTRODUCTION

Except for Ce, the local-moment magnetic state in elemental lanthanide metals is highly stable. Under the application of sufficient pressure, however, the magnetic state would be expected to destabilize. In recent studies on the trivalent lanthanide metals Nd [1], Gd [2], Tb [3], and Dy [2] the magnetic ordering temperature T_o, with the exception of Gd, was found to rise steeply to anomalously high values upon the application of extreme pressure. In the same pressure range, alloying Nd, Tb, and Dy in dilute concentration into superconducting Y resulted in a very large suppression of the superconducting transition temperature T_c, in the case of Y(Nd) the record value 39 K/(at.% Nd) [1]. Such high values are a signature of giant Kondo pair breaking, a sign that these lanthanides may be approaching a magnetic instability. The anomalous rise in T_o and the giant pair breaking thus appear to be related.

It is interesting to note that in the Kondo lattice model described by the Doniach phase diagram [4] T_o is expected to first increase with the magnitude of the negative covalent mixing exchange coupling J_- [5] before passing through a maximum and falling rapidly to the quantum critical point at 0 K (see Fig. 9). This occurs when the Ruderman-Kittel-Kasuya-Yosida (RKKY) interaction [6] is suppressed by Kondo spin screening. Since the magnitude of J_- normally increases under pressure [7], in the Doniach picture T_o versus pressure should pass through a maximum and fall towards 0 K. This behavior was indeed recently observed for elemental Nd metal by Song *et al.* [1]. In contrast, due to the extreme stability of Gd's magnetic state with its half-filled $4f^7$ configuration, even pressures to 1 or 2 Mbar are not sufficient to bring Gd near a magnetic instability. Indeed, neither giant pair breaking in Y(Gd) nor an anomalous rise in T_o for Gd are observed at extreme pressure [2,8].

In view of the intriguing magnetic behavior in trivalent Nd metal and Y(Nd) alloys at extreme pressure, an in-depth study of an additional light trivalent lanthanide Sm, both as elemental metal and in the dilute magnetic alloy Y(Sm), was undertaken. Sm metal crystallizes in the Sm-type (α-Sm)

structure at ambient pressure, transitioning to dhcp at 4 GPa, to fcc at 14 GPa, to $hR24$ (dfcc) at 19 GPa, to $hP3$ at 37 GPa, and finally to $tI2$ at 91 GPa [9,10]. These structural transitions thus follow the regular trivalent lanthanide structure sequence under pressure: hcp $\rightarrow$ Sm-type $\rightarrow$ dhcp $\rightarrow$ fcc $\rightarrow$ dfcc, a sequence generated by the increasing d character in the conduction band upon compression [11].

Trivalent Sm assumes the configuration [Xe]$4f^5$ yielding for the free Sm^{3+} ion in the ground state $^6H_{5/2}$, with Landé g-factor $g_J = 2/7$ and total angular momentum $J_t = 5/2$. The effective magnetic moment of free Sm^{3+} calculated from Hund's rules is $p_{eff} = 0.85 \mu_B$. However, magnetic susceptibility measurements on paramagnetic Sm salts give $p_{eff} = 1.74 \mu_B$ [12]. The difference between the theoretical and experimental values is believed due to contributions from low-lying excited states with different J_t values.

In Sm metal, the situation is more complicated since the crystalline electric field and conduction-electron polarization significantly influence the magnetic state of Sm^{3+} [13]. As a result of this complexity, Sm metal exhibits a number of interesting physical phenomena. Both the temperature-dependent heat capacity [14] and electrical resistivity [15] have anomalies near 13 and 106 K. The fact that the temperature-dependent magnetic susceptibility of Sm has peaks near these temperatures strongly suggests antiferromagnetic ordering [16]. This was confirmed by Koehler and Moon from neutron diffraction experiments on single crystalline ^{154}Sm [17]. They viewed the Sm-type structure with space group $R\bar{3}m$ as a combination of hexagonal and cubic sites where Sm^{3+} ions at these sites magnetically order at 106 and 14 K, respectively.

In temperature-dependent resistivity measurements $R(T)$, a knee is observed at the magnetic ordering temperature T_o due to the loss of spin-disorder scattering upon cooling. Dong *et al.* [18] measured resistivity on Sm to 43 GPa and found that the two ordering temperatures move toward each other with increasing pressure, finally merging together near 66 K at 8 GPa as Sm enters the dhcp phase. At higher pressures T_o increases rapidly to 135 K at 43 GPa. Johnson *et al.* [19] measured $R(T)$ on Sm to 47 GPa. They find that the two ordering temperatures merge near 56 K at 10 GPa and increase

slowly up to the ($hR24 \rightarrow hP3$) phase transition at 34 GPa where a second ordering temperature reportedly appears.

In this work, four-point dc resistivity measurements are carried out on pure Sm metal to ~150 GPa using a diamond anvil cell. The two magnetic ordering temperatures merge at 13 GPa after which $T_o(P)$ increases gradually to a maximum at 53 GPa, but then decreases and passes through a minimum at 85 GPa followed by a sharp increase to ~140 K at 150 GPa. Giant superconducting pair breaking is also observed in dilute Y(Sm) alloys. Taken together, both effects suggest that extreme pressure drives Sm to an unconventional magnetic state, a state likely related to that observed earlier in Nd, Tb, and Dy.

II. EXPERIMENTAL TECHNIQUES

Polycrystalline Sm samples for the high-pressure resistivity measurements were cut from a Sm ingot. The dilute magnetic alloys of Y(Sm) were made by argon arc-melting small amounts of Sm with Y (both Sm and Y 99.9% pure, Ames Laboratory [20]). To enhance homogeneity the alloys were sealed in glass ampules under vacuum and annealed at 600 °C for two weeks. The concentrations of Sm for the four alloys as determined from x-ray fluorescence analysis are: 0.15(2) at.%, 0.40(3) at.%, 0.83(4) at.%, and 1.16(6) at.%. Before arc-melting the nominal concentrations were 0.5 at.%, 1.0 at.%, 1.2 at.%, and 2 at.%, respectively. It follows that 30% to 70% of the Sm evaporated during arc-melting due to its relatively low boiling point.

A diamond anvil cell (DAC) made of conventional and binary CuBe [21] was used to reach pressures to ~150 GPa between two opposed diamond anvils (1/6-carat, type Ia) with 0.18 mm diameter culets beveled at 7° to 0.35 mm diameter. The force applied to the anvils was generated by a stainless-steel diaphragm filled with He gas [22]. The Re gasket (250 μm thick) was preindented to 30 μm and a 90 μm diameter hole drilled through the center of the preindentation area. A cBN-epoxy insulation layer was compressed onto the surface of the gasket. Four Pt strips (4 μm thick) were then placed on the insulation layer, acting as the electrical leads for the four-point resistivity measurement. The Sm or Y(Sm) sample with dimensions $40 \times 40 \times 4$ μm^3 was then placed on the Pt strips. Further details of the high-pressure resistivity techniques can be found elsewhere [2,23].

The DAC was inserted into an Oxford flow cryostat capable of varying temperature from ambient to 1.3 K. Pressure was determined at room temperature using the diamond vibron [24]. Earlier resistivity experiments by Song *et al.* [1] in an identical DAC using both vibron and ruby manometers revealed an approximately linear pressure increase of ~30% on cooling from 295 to 4 K. In the present experiments this calibration allows an estimate of the pressure at the magnetic or superconducting transition temperatures from the vibron pressure at ambient temperature.

III. RESULTS OF EXPERIMENT

Four-point resistance measurements $R(T)$ were carried out on Sm in two runs over the temperature and pressure ranges 1.3–295 K and 2–127 GPa (measured at room temperature),
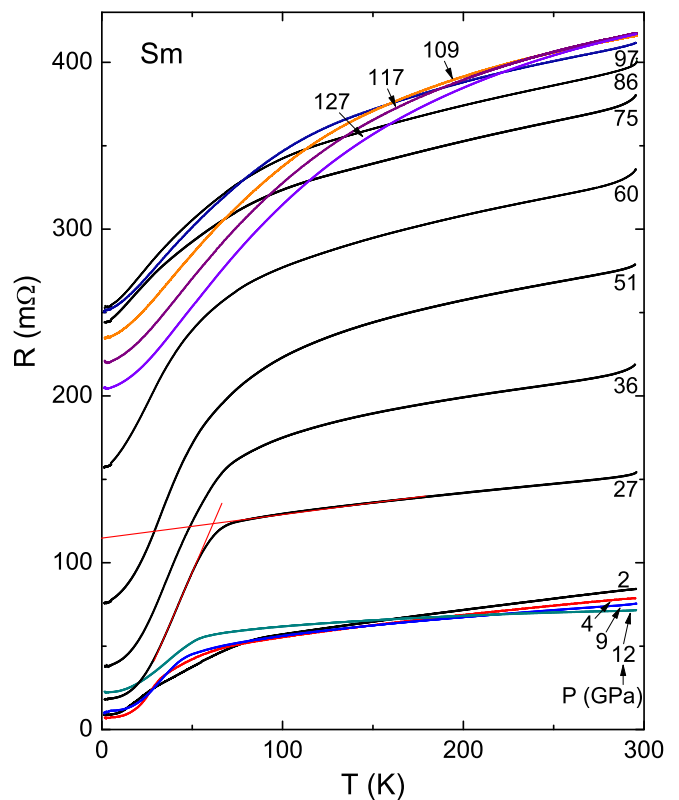

FIG. 1. Four-point resistance data $R(T)$ from run 1 for Sm metal vs temperature on warming from 1.3 to 295 K at multiple pressures to 127 GPa (measured at room temperature). Knee in $R(T)$ at T_o signals onset of magnetic order (for example, at 27 GPa $T_o \approx 61$ K). Straight red line fitting data above knee for 27 GPa intercepts resistance axis at 115 mΩ.

respectively. The data from run 1 are shown in Fig. 1. For all pressures, the resistance is seen to decrease upon cooling. A kink or knee appears in $R(T)$ in the lower temperature range that results from the progressive loss of spin-disorder scattering $R_{sd}(T)$ as Sm orders magnetically. At 2 and 4 GPa, two kinks are visible in the $R(T)$ curves; at higher pressures only one kink or knee appears. With increasing pressure the knee is seen to shift in temperature and broaden; the broadening is due to the increasing pressure gradient across the sample in the nonhydrostatic pressure environment. The value of T_o is determined from the intersection temperature of two straight lines tracking $R(T)$ above and below the knee region, as illustrated in Fig. 1 for 27 GPa pressure. In most experiments the Sm sample was cooled to ~4 K; however, considering both runs, at pressures 2, 9, 25, 51, 60, 86, 93, 97, and 127 GPa the sample was cooled to 1.3 K. In no experiment on Sm was superconductivity, or even an onset to superconductivity, observed.

In Fig. 2, the values of T_o for Sm from runs 1 and 2 are plotted versus pressure and compared to previous results from Dong *et al.* [18] to 43 GPa and Johnson *et al.* [19] to 47 GPa. In all experiments, the two branches of T_o are seen to merge near 13 GPa followed by an increase in T_o. In the present experiments, $T_o(P)$ passes through a maximum near 53 GPa, gradually decreasing to ~60 K near 85 GPa, before

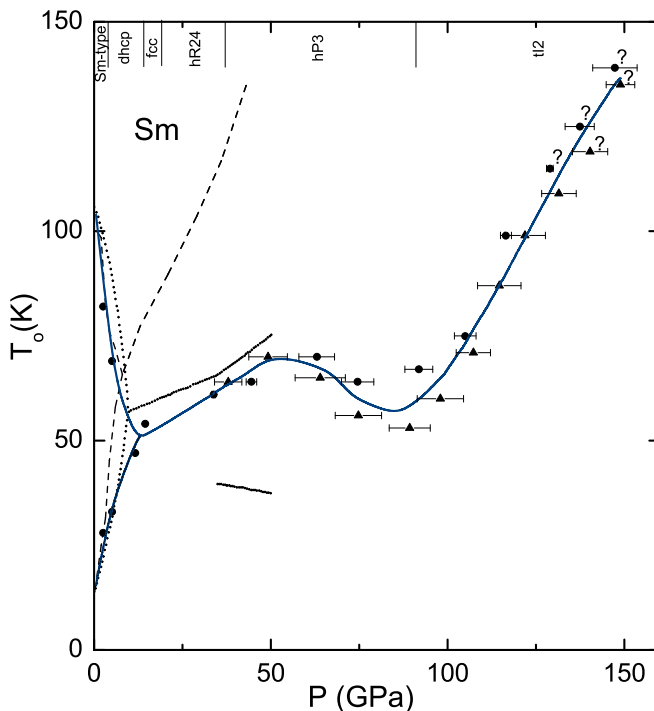FIG. 2. Magnetic ordering temperature T_o of Sm vs pressure. Data from run 1 (●), data from run 2 (▲), dotted line from Ref. [19], dashed line from Ref. [18]. Value of pressure is estimated for temperature near T_o (see text). Error bars give variation of pressure across sample. In run 1 below, 45 GPa error bars are smaller than symbol. Question marks (?) accompany data points where evidence for magnetic ordering is weak. Extended solid lines through data points are guides to the eye. Crystal structures for Sm at top of graph determined to 189 GPa [10].

FIG. 3. Plot of estimated maximum value of spin-disorder resistance $R_{sd}^{max}(P)$ vs pressure. R_{sd}^{max} is estimated by subtracting defect resistance R_d from intersection point R_{int} on resistance axis of straight-line fit to $R(T)$ data for $T > T_o$ (see text). Also shown is pressure dependence of $[R(290\,K) - R(4\,K)]$ using data from Fig. 1.

rising sharply to ∼140 K at 150 GPa. The report by Johnson *et al.* [19] that a second transition appears in the pressure range 35–50 GPa could not be confirmed.

Due to the broadening of the resistivity knee under nonhydrostatic pressure, the determination of the value of T_o for Sm becomes progressively more difficult in the upper pressure range. The same was true for the other trivalent lanthanides Nd, Gd, Tb, and Dy studied previously [1–3]. In particular, as here for Sm, a rapid upward shift of the knee in $R(T)$ was also observed for Dy above 70 GPa pressure [2]. That the knee for Dy does indeed result from magnetic ordering over the entire pressure range was recently confirmed by synchrotron Mössbauer spectroscopy (SMS) to 141 GPa [25].

Independent information on the origin of the resistivity knee in Sm can be gained by comparing the pressure dependence of the spin-disorder resistance $R_{sd}(P)$ for $T > T_o$ to that of $T_o(P)$ obtained from the resistivity knee. As discussed in Ref. [2], both T_o [26] and R_{sd} [27] are proportional to $J^2 N(E_F)$, where J is the exchange interaction between local moment and conduction electrons and $N(E_F)$ is the density of states at the Fermi energy. A similarity between the pressure dependencies $T_o(P)$ and $R_{sd}(P)$ is anticipated for the trivalent lanthanide metals since their spd conduction electron properties are closely related. This similarity was indeed observed for Nd [1], Gd [2], Tb [3], and Dy [2]; it would be interesting to
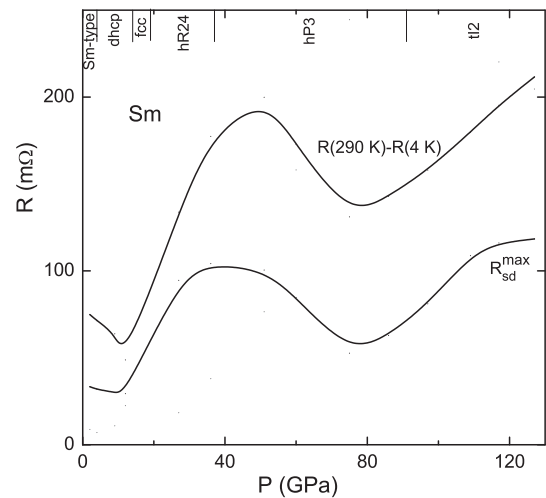
examine whether this also holds for Sm, together with Nd the second light lanthanide studied. From Fig. 1, it is readily seen that where the resistivity knee shifts under pressure to higher temperatures the size of the resistivity drop-off below the knee also increases. A semi-quantitative estimate of R_{sd} is now attempted.

The total measured resistance is the sum of three terms, $R(T) = R_d + R_{ph}(T) + R_{sd}(T)$, where $R_d = R(0\,K)$ is the temperature-independent defect contribution. In the paramagnetic state in the temperature region above the resistance knee, $R_{sd}(T)$ is constant, taking on its maximum value R_{sd}^{max}, so that the only temperature dependence comes from the phonon resistance $R_{ph}(T)$. To estimate R_{sd}^{max}, Colvin *et al.* [28] assumed that $R_{ph}(T)$ depends linearly on temperature, and extended a straight line fit to $R(T)$ for $T > T_o$ to 0 K with intercept R_{int} and then subtracted off R_d from this intercept. An example for this estimate is given in Fig. 1 at 27 GPa, where $R_{sd}^{max} = [R_{int} - R_d] = (115 - 18)\,m\Omega = 97\,m\Omega$.

In Fig. 3, R_{sd}^{max} is plotted as a function of pressure. Comparing Figs. 2 and 3, a parallel behavior of the pressure dependences $T_o(P)$ and $R_{sd}^{max}(P)$ is indeed observed, thus supporting the identification of the resistance knee with the onset of magnetic ordering in Sm. Also included in Fig. 3 is the quantity $[R(290\,K)–R(4\,K)]$ that is seen to also qualitatively track T_o versus pressure. This suggests that the resistance from electron-phonon scattering at room temperature does not change dramatically within the pressure range of these experiments.

To examine whether the rapid rise in T_o for pressures above 85 GPa might be related to an approaching instability in Sm's magnetic state, Sm is alloyed in dilute concentration with Y, a high-pressure superconductor having, compared to the trivalent lanthanides, closely similar conduction electron properties and structural sequence under pressure [29]. Under these circumstances the ability of the Sm ion to suppress Y's superconductivity, the degree of pair breaking
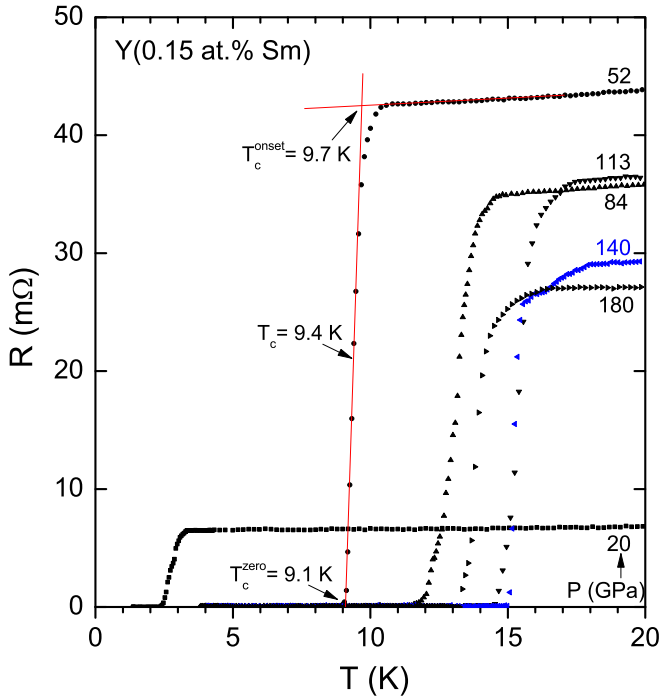
FIG. 4. Four-point resistance of Y(0.15 at.% Sm) alloy vs temperature showing superconducting transition at various pressures to 180 GPa (estimated at low temperature). Intersection of two red straight lines defines T_c^{onset}, midpoint of transition defines T_c, temperature where $R(T) \simeq 0$ defines T_c^{zero}.
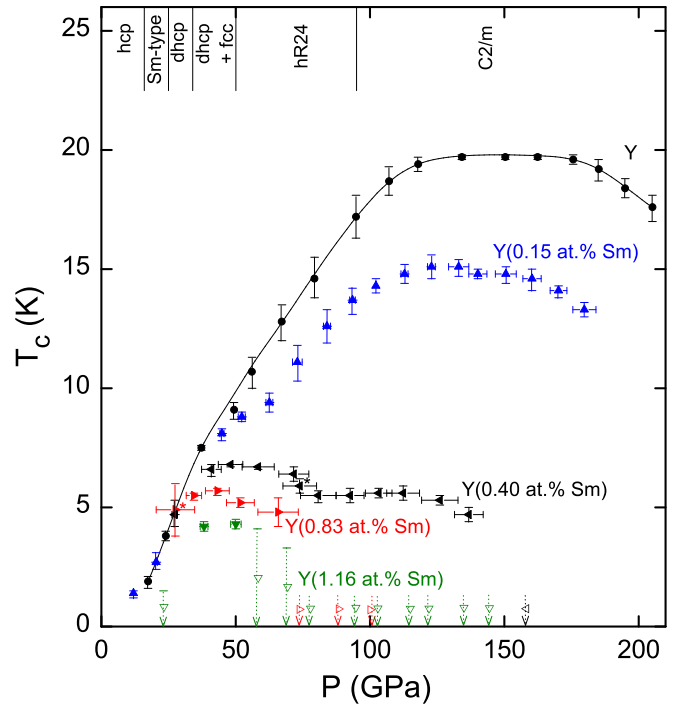

FIG. 5. Superconducting transition temperature T_c vs pressure (estimated at low temperature) for Y and Y(Sm) alloys at four different Sm concentrations. Error bars give (vertical) uncertainty in T_c values and (horizontal) variation of pressure across sample. In all cases, giant superconducting pair breaking $\Delta T_c \equiv T_c[\text{Y}] - T_c[\text{Y(Sm)}]$ is observed. At top of graph, are crystal structures for superconducting host Y to 177 GPa [31].

$\Delta T_c \equiv T_c[\text{Y}] - T_c[\text{Y(Sm)}]$, can reveal valuable information about the magnetic state of the Sm ion itself. This general observation was emphasized for lanthanide ions by Maple [30].

In the present experiment, Y(Sm) alloys with differing dilute Sm concentrations were studied at pressures to 180 GPa. Figure 4 shows the superconducting transitions in four-point resistance measurements on Y(0.15 at.% Sm) at selected pressures. As illustrated in this figure for the $R(T)$ data at 52 GPa, T_c is defined as the temperature at which the resistance transition reaches the halfway mark, whereas the intersection point of two straight red lines defines T_c^{onset}, and T_c^{zero} gives the temperature where the resistance disappears. The fact that a typical total transition width is less than 2 K gives evidence that the distribution of Sm ions in the alloys is homogeneous. As seen from the data in Fig. 4, T_c increases monotonically with pressure to 140 GPa, but then decreases to 180 GPa.

The dependence of T_c on pressure for Y(Sm) alloys with Sm concentrations 0.15, 0.40, 0.83, and 1.16 at.% is shown in Fig. 5. Below ~40 GPa the $T_c(P)$ dependence for all four alloys tracks that for pure Y. However, above ~40 GPa a strong suppression sets in. This suppression ΔT_c is so strong that for Y(1.16 at.% Sm) at pressures above 50 GPa T_c lies below the temperature range of this experiment (1.3 K). For the more dilute Y(0.15 at.% Sm) and Y(0.40 at.% Sm) alloys, T_c remains well above 1.3 K at all pressures.

To allow a more meaningful comparison of the degree of superconducting pair breaking ΔT_c for the different alloys, in Fig. 6, ΔT_c is divided by the Sm concentration c and then

plotted versus pressure for all alloys measured. Where they can be compared, the individual $\Delta T_c/c$ curves agree reasonably well and increase monotonically with pressure, reaching the extremely high value of ~40 K/at.% Sm at 180 GPa, a value slightly higher than that found earlier for Y(0.4 at.% Nd) [1]. Both the giant pair breaking in Y(Sm) and the remarkable increase of T_o in Sm give evidence for unconventional physics in Sm above 85 GPa.

IV. DISCUSSION

The present results on Sm and Y(Sm) alloys will now be compared to those from earlier studies on the lanthanides Nd [1], Gd [2], Tb [3], and Dy [2]. Going from right to left across the lanthanide series (Lu to La) or by applying pressure, one finds with few exceptions [31] the canonical rare-earth crystal structure sequence hcp $\rightarrow$ Sm-type $\rightarrow$ dhcp $\rightarrow$ fcc $\rightarrow$ hR24 believed to mainly arise from an increase in the number n_d of d electrons in the conduction band [11].

In the elemental lanthanide metals, magnetic ordering arises from the indirect RKKY exchange interaction between the magnetic ions. For a conventional lanthanide metal with a stable magnetic moment, the magnetic ordering temperature T_o is expected to scale with the de Gennes factor $(g-1)^2 J_t(J_t + 1)$, modulated by the prefactor $J^2 N(E_F)$, where J is the exchange interaction between the $4f$ ion and the conduction electrons, $N(E_F)$ the density of states at the Fermi energy,
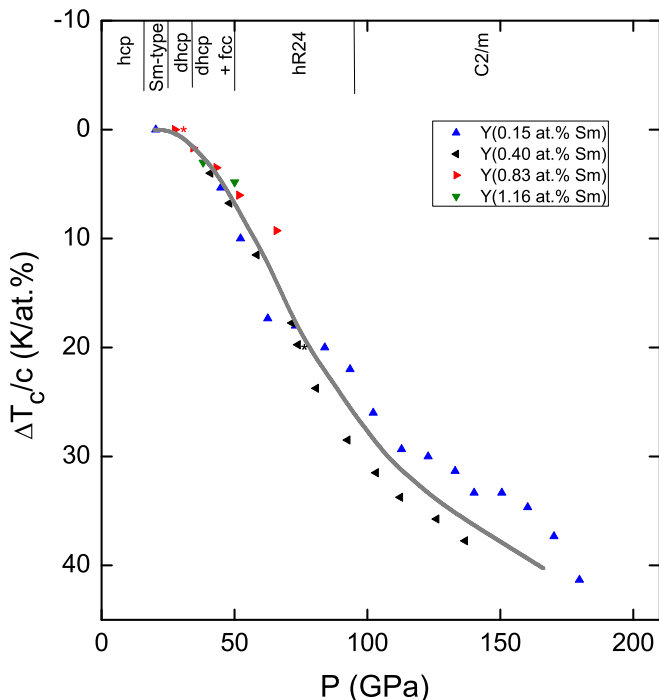
FIG. 6. Superconducting pair breaking ΔT_c divided by concentration c of Sm in four Y(Sm) alloys plotted vs pressure. At top of graph are crystal structures for superconducting host Y to 177 GPa [31]. Line through data is guide to the eye.

g the Landé-g factor, and J_t the total angular momentum quantum number [26].

In Fig. 7(a), the dependence of the magnetic ordering temperature T_o on pressure is shown for the four lanthanide metals Nd, Sm, Tb, and Dy. Except for Nd, $T_o(P)$ is seen to initially decrease rapidly with pressure, but then pass through a minimum and rise. $T_o(P)$ for Gd [2] also shows this same initial behavior. Since the de Gennes factor, in the absence of a magnetic instability or valence transition, is constant under pressure, the initial $T_o(P)$ dependence for the above lanthanides likely originates in the pressure dependence of the prefactor $J^2 N(E_F)$. Electronic structure calculations for Dy support this conclusion [32,33].

The strong initial decrease in T_o with pressure in Sm (upper transition), Gd, Tb, and Dy occurs within the hcp and Sm-type phases. The minimum in $T_o(P)$ at approximately 20 GPa for Dy appears at somewhat lower pressures for Tb, Gd, and Sm, disappearing entirely for Nd. As discussed in some detail in Ref. [1], this is consistent with an increase in the number of d electrons in the conduction band going from Dy to Nd; the electronic structure and the crystal structures taken on by Nd resemble those of Dy but at a pressure approximately 30–40 GPa higher [1]. The systematic behavior for all five lanthanides Dy, Tb, Gd, Sm, and Nd in the region of pressure where the hcp, Sm-type, dhcp, and $hR24$ structures occur, gives evidence that changes in the magnetic ordering temperature in this region are mainly determined by corresponding changes in the properties of the conduction electrons that mediate the RKKY interactions between the magnetic lanthanide ions. At higher pressures
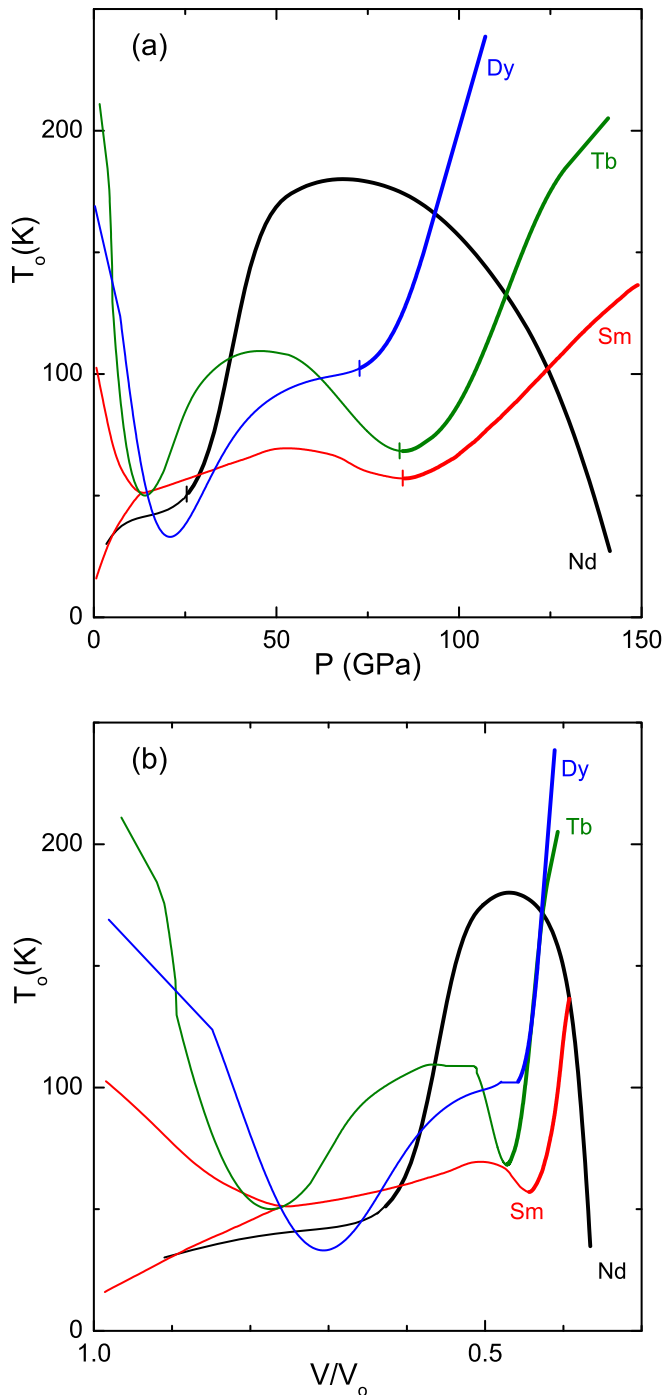

FIG. 7. (a) Graph comparing lines through T_o vs pressure data for Nd, Sm, Tb, and Dy. Vertical tick marks and double line width signal beginning of region with anomalous rapid rise in T_o with pressure. (b) Data in (a) are replotted vs V/V_o, where V_o is sample volume at ambient pressure, using measured equations of state of Nd [34], Sm [9], Tb [35], and Dy [36].

the above lanthanides, with the exception of Gd, transform from $hR24$ to lower-symmetry structures accompanied by an anomalous pressure dependence of the magnetic ordering temperature $T_o(P)$.

It would seem helpful to propose that the $T_o(P)$ curves for each lanthanide can be separated into two principal pressure

regions: a "conventional" region at lower pressure within the hcp, Sm-type, dhcp, and $hR24$ structures governed by the electronic properties of the conduction electrons and normal positive exchange interactions J_+ between the lanthanide ion and the conduction electrons, and an "unconventional" region at higher pressures where exotic physics dominates leading to negative covalent-mixing exchange J_- and associated anomalous magnetic properties. In the "conventional" region, the observed variations in $T_o(P)$ would be principally caused by changes in the prefactor $N(E_F)J_+^2$ with pressure. In the "unconventional" pressure region, highly correlated electron effects dominate leading to anomalous magnetic properties, including anomalous $T_o(P)$ dependencies, such as its rapid rise, and the beginning of large superconducting pair breaking in the dilute magnetic alloys.

Although the properties of the conduction electrons and the magnetic state of the lanthanide ion are intertwined, the "conventional" and "unconventional" regions represent different physics, the former being amenable through standard electronic structure calculations, whereas the latter is only accessible through consideration of strong highly correlated electron effects. The stability of the ion's magnetic state is determined to a large extent by the exchange interactions *within* a given lanthanide ion (Hund's rules). Once the "unconventional" dependence in T_o on pressure sets in, it overpowers the "conventional" conduction electron behavior and determines $T_o(P)$.

Focussing now on the anomalous rise in T_o with pressure beginning at the vertical tick mark in Fig. 7(a), we note that this rise is steepest for Nd but becomes progressively less steep for Dy, Tb, and Sm. At least part of this reduction in steepness has to do with the fact that the compressibility of the lanthanides decreases significantly as pressure is increased. To bring out the physics more clearly, T_o in Fig. 7(b) is replotted versus the relative volume V/V_o. Different features in the respective curves are shifted to new relative positions, but now it is seen that the sharp upturns in $T_o(P)$ have nearly the same slope and are much steeper relative to the changes in the "conventional" region at lower pressures. This points to a common mechanism for the upturn in these four lanthanides.

In Fig. 8 the normalized pair breaking curve $\Delta T_c/c$ for Y(Sm) from Fig. 6 is compared to those for the dilute magnetic alloys Y(Nd) [1], Y(Tb) [3], and Y(Dy) [2]. For Y(Sm) and Y(Nd) the pair breaking begins to increase rapidly at relatively low pressures compared to Y(Tb) and especially Y(Dy). At least part of the reason for this is that the Y host exerts lattice pressure on the light lanthanides Sm and Nd, but not on Tb and Dy. This can be seen by comparing the respective molar volumes in units of cm³/mol: Y(19.88), Nd(20.58), Sm(19.98), Gd(19.90), Tb(19.30), and Dy(19.01) [37]. Without exception, the region of pressure where $T_o(P)$ increases rapidly lies within the region of pressure where superconducting pair breaking $\Delta T_c/c$ in the corresponding dilute magnetic alloy with Y is anomalously large. Note also that the maximum value of the slope of $\Delta T_c/c$ versus pressure in Fig. 8 is noticeably reduced for Y(Dy). At least part of this effect is due to the sizable reduction in the compressibility of Y at higher pressures.

For the dilute magnetic alloy Y(Nd), the normalized pair breaking data in Fig. 8 are seen to be reduced ($\Delta T_c/c$ turns
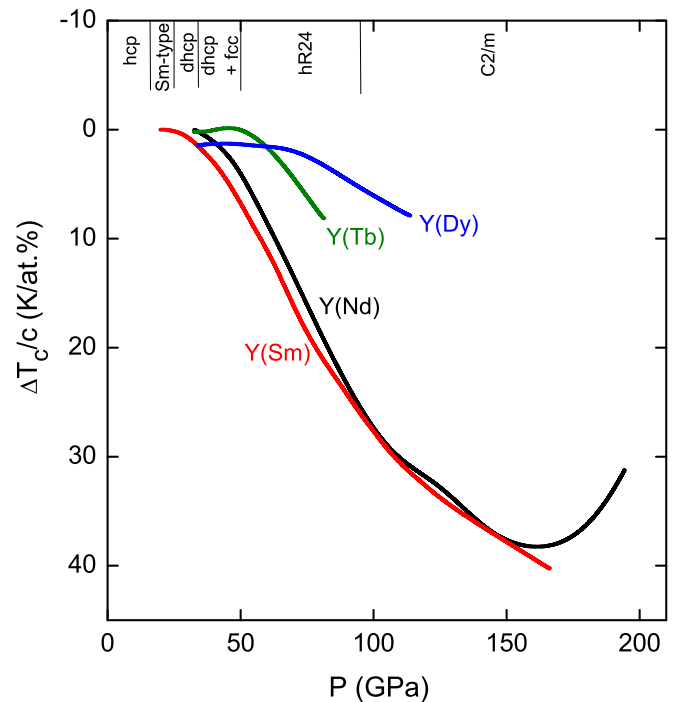

FIG. 8. Graph comparing relative superconducting pair breaking $\Delta T_c/c$ for dilute magnetic alloys Y(Nd), Y(Sm), Y(Tb), and Y(Dy) vs pressure showing lines through data as in Fig. 6 for Y(Sm). At the top of the graph, crystal structures for superconducting host Y to 177 GPa [31] are given.

upwards) for pressures above 160 GPa. Presumably the same effect would also be observed in Y(Sm), Y(Tb), and Y(Dy) if the experiments were extended to even higher pressures. This reduction in giant pair breaking seen in Y(Nd) at the highest pressures was observed previously in dilute magnetic alloys La(Ce) [38], La(Pr) [39], and Y(Pr) [8,40] and can be readily accounted for in terms of Kondo pair-breaking theory [41] where the magnitude of the negative exchange interaction J_- between the magnetic ions and the conduction electrons increases with pressure. The appearance of such Kondo physics in the dilute magnetic alloy suggests that the corresponding concentrated system will likely show Kondo lattice, heavy fermion, and fluctuating valence behavior at higher pressures, eventually culminating in a full increase in valence whereby one $4f$ electron completely leaves its orbital and joins the conduction band.

The well known Doniach model [4] is often cited to account for the dependence of the magnetic ordering temperature T_o in a Kondo lattice as a function of the magnitude of the negative exchange parameter J_- (see Fig. 9). Whereas the upturn in $\Delta T_c/c$ occurs above 160 GPa for Y(Nd), the downturn in $T_o(P)$ begins above 80 GPa [see Fig. 7(a)] for Nd. The rapid rise in $T_o(P)$ for Nd followed by its rapid downturn resembles the dependence anticipated from the Doniach model [1]. A similar $T_o(P)$ dependence would be expected for Sm, Tb, and Dy if the experiments were extended to even higher pressures.

The values of the pair-breaking parameter $\Delta T_c/c$ for Nd and Sm impurities in Y are surprisingly large—in fact, to our knowledge, the largest ever reported. However, even more surprising is the sharp upturn in $T_o(P)$, where T_o reaches values
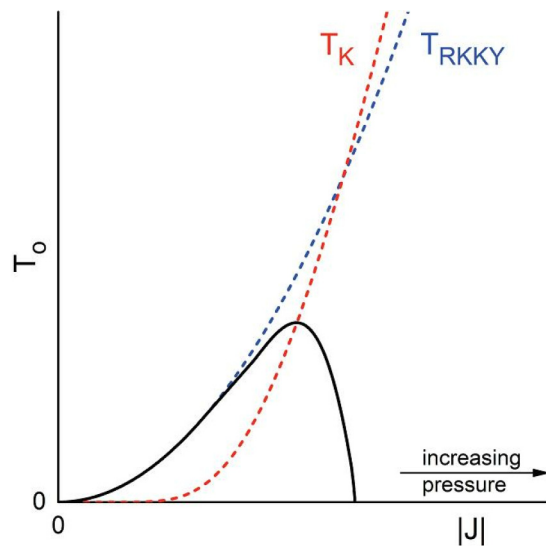
FIG. 9. Magnetic ordering temperature T_o vs absolute value of negative exchange parameter J according to the Doniach model [4]. Since T_o from the RKKY interaction increases as J^2, but is overtaken by the exponential increase of the Kondo temperature T_K, the magnetic ordering is quenched.

that appear to be much higher than would have been possible had "unconventional" physics, such as Kondo physics, not

been operative. In the case of Dy, $T_o(P)$ extrapolates to values well above room temperature, higher than any known value for an elemental lanthanide metal at either ambient or high pressure [2].

In summary, the magnetic properties of the light lanthanide Sm have been studied to extreme pressure and found to parallel those of another light lanthanide, Nd, as well as the heavy lanthanides Gd, Tb, and Dy. It appears that the magnetic phase diagram can be separated into two regions: a low-pressure region where conventional changes in the electronic structure determine $T_o(P)$, and a high-pressure region where highly correlated electron effects dominate, leading to such anomalous phenomena as unexpectedly high magnetic ordering temperatures and giant superconducting pair breaking. The authors hope that this and previous work will lead to increased theoretical activity in this area.

ACKNOWLEDGMENTS

[1] J. Song, W. Bi, D. Haskel, and J. S. Schilling, Phys. Rev. B **95**, 205138 (2017).

[2] J. Lim, G. Fabbris, D. Haskel, and J. S. Schilling, Phys. Rev. B **91**, 045116 (2015).

[3] J. Lim, G. Fabbris, D. Haskel, and J. S. Schilling, Phys. Rev. B **91**, 174428 (2015).

[4] S. Doniach, in *Valence Instabilities and Related Narrow-Band Phenomena*, edited by R. D. Parks (Plenum, New York, 1977), p. 169; S. Doniach, Physica B+C **91**, 231 (1977).

[5] J. R. Schrieffer, J. Appl. Phys. **38**, 1143 (1967).

[6] M. A. Ruderman and C. Kittel, Phys. Rev. **96**, 99 (1954).

[7] J. S. Schilling, Adv. Phys. **28**, 657 (1979).

[8] G. Fabbris, T. Matsuoka, J. Lim, J. R. L. Mardegan, K. Shimizu, D. Haskel, and J. S. Schilling, Phys. Rev. B **88**, 245103 (2013).

[9] Y. C. Zhao, F. Porsch, and W. B. Holzapfel, Phys. Rev. B **50**, 6603 (1994).

[10] Y. Vohra, L. Akella, S. Weir, and G. A. Smith, Phys. Lett. A **158**, 89 (1991).

[11] J. C. Duthie and D. G. Pettifor, Phys. Rev. Lett. **38**, 564 (1977).

[12] S. Blundell, in *Magnetism in Condensed Matter* (Oxford University Press, New York, 2001), p. 34.

[13] H. Adachi, H. Ino, and H. Miwa, Phys. Rev. B **56**, 349 (1997).

[14] L. D. Jennings, E. D. Hill, and F. H. Spedding, J. Chem. Phys. **31**, 1240 (1959).

[15] J. K. Alstad, R. V. Colvin, S. Legvold, and F. H. Spedding, Phys. Rev. **121**, 1637 (1961).

[16] K. A. McEwen, P. F. Touborg, G. J. Cock, and L. W. Roeland, J. Phys. F **4**, 2264 (1974).

[17] W. C. Koehler and R. M. Moon, Phys. Rev. Lett. **29**, 1468 (1972).

[18] W. Y. Dong, T. H. Lin, K. J. Dunn, and C. N. J. Wagner, Phys. Rev. B **35**, 966 (1987).

[19] C. R. Johnson, G. M. Tsoi, and Y. K. Vohra, J. Phys.: Condens. Matter **29**, 065801 (2017).

[20] Material Preparation Center, Ames Laboratory, U. S. Department of Energy, Ames, Iowa, http://www.mpc.ameslab.gov.

[21] J. S. Schilling, in *Proceedings of the 9th AIRAPT International High Pressure Conference*, Albany, New York, July 24-29, 1983, edited by C. Homan, R. K. MacCrone and E. Whalley (North-Holland, New York, 1984); J. S. Schilling, Mater. Res. Soc. Symp. Proc. **22**, 79 (1984).

[22] W. B. Daniels and W. Ryschkewitsch, Rev. Sci. Instrum. **54**, 115 (1983).

[23] K. Shimizu, K. Amaya, and N. Suzuki, J. Phys. Soc. Jpn. **74**, 1345 (2005).

[24] Y. Akahama and H. Kawamura, J. Appl. Phys. **100**, 043516 (2006).

[25] W. Bi, J. Song, Y. Deng, P. Materne, J. Zhao, E. E. Alp, M. Y. Hu, D. Haskel, Y. Lee, and J. S. Schilling (unpublished).

[26] See, for example, K. N. R. Taylor and M. I. Darby, *Physics of Rare Earth Solids* (Chapman and Hall, London, 1972).

[27] H. J. van Daal and K. H. J. Buschow, Solid State Commun. **7**, 217 (1969).

[28] R. V. Colvin, S. Legvold, and F. H. Spedding, Phys. Rev. **120**, 741 (1960).

[29] J. Wittig, Phys. Rev. Lett. **24**, 812 (1970); J. J. Hamlin, V. G. Tissen, and J. S. Schilling, Physica C (Amsterdam) **451**, 82 (2007).

[30] M. B. Maple, Appl. Phys. **9**, 179 (1976).

[31] G. K. Samudrala, G. M. Tsoi, and Y. K. Vohra, J. Phys.: Condens. Matter **24**, 362201 (2012).

[32] D. D. Jackson, V. Malba, S. T. Weir, P. A. Baker, and Y. K. Vohra, Phys. Rev. B **71**, 184416 (2005).

[33] G. S. Fleming and S. H. Liu, Phys. Rev. B **2**, 164 (1970); S. H. Liu, Phys. Rev. **127**, 1889 (1962).

[34] G. N. Chesnut and Y. K. Vohra, Phys. Rev. B **61**, R3768 (2000).

[35] N. C. Cunningham, W. Qiu, K. M. Hope, H.-P. Liermann, and Y. K. Vohra, Phys. Rev. B **76**, 212101 (2007).

[36] R. Patterson, C. K. Saw, and J. Akella, J. Appl. Phys. **95**, 5443 (2004).

[37] C. N. Singman, J. Chem. Ed. **61**, 137 (1984).

[38] M. Maple, J. Wittig, and K. Kim, Phys. Rev. Lett. **23**, 1375 (1969).

[39] J. Wittig, Phys. Rev. Lett. **46**, 1431 (1981).

[40] J. Wittig, *Valence Instabilities*, edited by P. Wachter and H. Boppart (North-Holland, Amsterdam, 1982), p. 427.

[41] M. Zuckermann, Phys. Rev. **168**, 390 (1968); E. Müller-Hartmann and J. Zittartz, Z. Phys. **234**, 58 (1970).